JCE

Journal of Civil Engineering
ISSN 2086 - 1206 E-ISSN 2579 - 9029

An Experiment of Shear Strength Reinforced Geopolymer Concrete Beam Based High-Calcium Fly Ash with Varian Shear Span-to-Depth Ratio

Moh. Safi'i Mansur[a*], Priyo Suprobo[b], Yuyun Tajunnisa[c], Auliagitta Kumala Apsari[d]

Correspondence

[a]Master Student in the Civil Engineering Department, Institut Teknologi Sepuluh Nopember, ITS Campus, Sukolilo, Surabaya 60111, Indonesia.
[b]Lecturer in the Civil Engineering Department, Institut Teknologi Sepuluh Nopember, ITS Campus, Sukolilo, Surabaya 60111, Indonesia.
[c]Lecturer in the Civil Infrastructure Engineering Department, Institut Teknologi Sepuluh Nopember, ITS Campus, Manyar, Surabaya 60282, Indonesia.
[d]Bachelor Student in the Civil Infrastructure Engineering Department, Institut Teknologi Sepuluh Nopember, ITS Campus, Manyar, Surabaya 60282, Indonesia.

Corresponding author email address:
mohsafiimansur@gmail.com

Submitted : 03 July 2023
Revised : 01 September 2023
Accepted : 04 September 2023

Abstract

This study discusses geopolymer-reinforced concrete beam's shear strength capacity by experimental observation using high-calcium fly ash as the main binder. This study observed the influence of shear span per effective depth ratio due to the geopolymer concrete beam's shear behavior and strength capacity. Two beams are designed to have diagonal tensile cracks; hence the shear failure state could be obtained. Each beam has similar properties by 150 mm in width, 250 mm in height, 1800 mm in length, 2D16 as the flexure bar reinforcement, and stirrups of Ø6-250 with 20 mm concrete cover. The research employed the four-point load bending testing with the load span difference of each beam, which will later be the study variable. The beam A has a load span ratio a/d 2 and the beam B has a/d 2.5. The things sought in this study include the peak load-deflection curve, the shear capacity that occurs in geopolymer concrete beams, and the shear capacity comparison with ACI 318-19. The results of the tests that have been carried out show that type A geopolymer-reinforced concrete beam was more ductile than type B beams, with a percentage difference of about 21.49% in deflection. The shear strength at the ratio a/d of 2 was 115,04 kN, and the ratio a/d of 2.5 was 89,00 kN. As well as a comparison of the shear strength of the test results with calculations according to ACI 318-19 shows a ratio of 1.69. So it can be concluded that ACI 318-19 calculations were conservative.

Keywords

Geopolymer concrete, high-calcium fly ash, shear strength, a/d ratio

INTRODUCTION

One of the significant environmental problems of concrete-based building materials is the high carbon dioxide emissions that arise during cement manufacture [1]. The cement industry contributes about 5% of global carbon dioxide emissions [2]. On the other hand, high infrastructure development also impacts the increasing demand for cement needs [3]. This problem must be overcome immediately by reducing the use of cement and using more environmentally friendly materials [4]. Geopolymer concrete is one of the environmentally friendly concrete whose constituent materials do not use cement [5]. Previous research has discovered geopolymer concrete's structural and mechanical behavior on slab, column, and beam elements [6]–[9]. However, most of these studies used low-calcium fly ash [10]–[13]. Therefore, more research is needed on the mechanical properties of geopolymer concrete that contains high-calcium fly ash, despite the increasing availability of fly ash waste, particularly type C. This issue can be attributed to the use of low-quality coal that produces type F fly ash waste as an alternative energy source for oil and gas in recent decades, which has resulted in a shortage of high-quality coal with Type F fly ash as byproduct waste [14]. Hence this research was conducted to obtain the structural behavior of geopolymer concrete using high-calcium fly ash as the main binder alternative.

RESEARCH SIGNIFICANCE

This study aims to determine the shear behavior and the strength capacity of the geopolymer-reinforced concrete beam based on high calcium fly ash with different loading spans (a/d).

METHODOLOGY

The method used in this study was by experimenting on geopolymer-reinforced concrete beams based on high calcium fly ash with a size of 250x150x1800 mm. The main discussion in this study was load-deflection curves, cracking patterns that occur, shear capacity, and comparison of shear capacity with analytical calculations following ACI 318-19.

A. MATERIAL PREPARATION

In this step, material testing was performed to determine the characteristics of each used material. The mix design

proportion of geopolymer concrete will be affected by material characteristics, such as:

A.1. FLY ASH

This study uses type C fly ash as the binder alternative. Several tests identified the objectives of the type C fly ash, such as the XRF test (X-ray fluorescence) to determine the calcium levels according to ASTM C618-15 and the XRD test (X-ray Diffraction) to identify the crystal grains in fly ash. The tests required for alkaline activators are specific gravity tests for NaOH according to the molarity and sodium metasilicate gravimetric tests. This study used 12Molar of NaOH because of the maximum compressive strength ability without ruining the standard deviation value [15]. Table 3 and Table 4 shows the result of these tests.

Table 1 and Table 2 show the result of these tests.

A.2. ALKALINE-ACTIVATOR

This material is used to conduct the polymerization process of the binder. NaOH was chosen as the alkaline activator due to the Na^+ ions that were found to be more reactive [16]. NaOH will react to the Silicate and Aluminum contained in fly ash to form the polymer bond stability. In addition to NaOH, the alkaline activator material used is Sodium Metasilicate Pentahydrate, which accelerates the polymerization of geopolymer concrete [17]. The tests required for alkaline activators are specific gravity tests for NaOH according to the molarity and sodium metasilicate gravimetric tests. This study used 12Molar of NaOH because of the maximum compressive strength ability without ruining the standard deviation value [15]. Table 3 and Table 4 shows the result of these tests.

Table 1 XRF test result

Oxide Content (%)			
CaO	17.79	SO_3	1.39
SiO_2	37.94	K_2O	1.15
Al_2O_3	14.29	Na_2O	1.42
Fe_2O_3	15.45	TiO_2	0.84
MgO	7.12	P_2O5	0.18
LOI (%) 0.15			

Table 2 XRD test result

Solid Particles	Percentage (%)
Quartz	6,802
Brownmillerite (Si, Mg)	1,105
Periclase	3,748
C3A Na orthorhombic	0,463
C3A Cubic	1,106
C3A monoclinic	0,435
C3A Na Cubic	2,362
C3Aftrans	2,100
C3F (Colville)	0,676
Anhydrate	1,239
Magnetite	1,187
Spinel	1,819
Akermanite	0,001
Arcanite K2SO4	0,071
Lime	0,273
Maghemite	2,157
Ferrochrome	1,158
Amorphous	7,330

Table 3 Specific gravity test result

Parameters	Sample 1	Sample 2	Sample 3
Piknometer 1000 ml (gr)	248,4	266,9	265,6
NaOH (gr)	480	480	480
Piknometer + NaOH solution (gr)	1557,3	1613,4	1606,3
Specific gravity	1308,9	1346,5	1340,7
Average	1332,03 kg/cm^3		

Table 4 Gravimetry test result

Na_2SiO_3			Total
H_2O	Na_2O	SiO_2	
46,44%	18,71%	21,7%	86,85%

A.3. COARSE AGGREGATES

The coarse aggregate used in this study was crushed stone (gravel) with a maximum size of 20 mm. The size of the coarse aggregate affects the calculation of the mix design proportion. Several tests that occurred are sieve analysis (ASTM C135), bulk density & voids in aggregates (ASTM C29/C 29M), also absorption degree (ASTM C127-15), and moisture content (ASTM C566-97) [18].

Table 5 Sieve grading analysis of coarse aggregates

Num.	Restained weight	% Restained	Cumulative restained	% material passing
1 ½ "	0	0	0	100
¾ "	32,80	0,21	0,21	99,79
½ "	10240,00	64,11	64,32	35,68
3/8"	5353,00	33,51	97,83	2,17
Pan	346,30	2,17	100,00	0,00
Sum	15972,10	100,00	751,51	237,65
FKr			7,52 %	

Per the grading standard, each material passing the sieve number constructs the result classified as zone 1-4. The Table 5 result is presented in Figure 1.

Table 6 Coarse aggregates bulk density

Parameters	Sample A	Sample B	Sample C
Saturated Surface Dry (gr)	3000,2	3001,3	3000,8
Weight in the water (gr)	1894,6	1894,5	1891,2
Bulk density (gr/cm^3)	2,714	2,712	2,704
Average bulk density	2,710 gr/cm^3		

Table 7 Water absorption degree of coarse aggregates

Parameters	**Sample A**	**Sample B**
Saturated Surface Dry (gr)	3000,2	3001,3
Oven-dried weight (gr)	2954,5	2956,2
Water absorption degree	1,55%	1,53%
Average water absorption	1,54%	

Table 8 Moisture content in coarse aggregates

Parameters	Sample A	Sample B
Aggregates	1001,7	1001,1
Oven-dried	986,6	984,8
Water moisture	1,53	1,65
Average moisture content	1,59%	

A.4. FINE AGGREGATES

Fine aggregates used in this study have a grain size of less than 3/16 inches, or that passes filter number 4. Fine

aggregate testing includes sieve analysis, specific gravity, absorption, and moisture content.

Table 9 Sieve grading analysis of fine aggregates

Num.	Restained weight	% Restained	Cumulative restained	% Material passing
4,76	0,3	0,03	0,03	99,97
2,38	38,1	3,82	3,85	96,15
1,19	156,3	15,68	19,53	80,47
0,6	148,6	14,91	34,44	65,56
0,3	332,8	33,39	67,83	32,17
0,15	251,7	25,25	93,08	6,92
0,075		0,00	93,08	6,92
Pan	69	6,92	100,00	0,00
Sum	996,8	100,00	311,84	388,16
FKr			3,12%	

Table 10 Fine aggregates bulk density

Parameters	Sample A	Sample B	Sample C
SSD fine agg (gr)	500,2	500,5	500,5
Measuring flask 1000 cc (gr)	265,7	248,5	265,7
Water and fine agg in the flask (gr)	1577,9	1561,1	1578,2
Water (gr)	1262,3	1241,7	1259,3
Spec grav of fine agg	2,709	2,763	2,756
Average of specific gravity	2,743 gr/cm^3		

Table 11 Water absorption degree of fine aggregates

Parameters	Sample A	Sample B
Saturated Surface Dry (gr)	500,6	500,5
Oven-dried weight (gr)	499,6	500,3
Water absorption degree	0,20%	0,040%
Average water absorption	1,20%	

Table 12 Moisture content in fine aggregates

Parameters	**Sample A**	**Sample B**	**Sample C**
Aggregates (gr)	500,5	500,2	500,1
Oven-dried (gr)	469,5	470,9	470,4
Water moisture (%)	6,60	6,22	6,31
Average moisture content		6,38%	

A.5. SUPERPLASTICIZER

This material is identified as an admixture. The type of admixture used in this study is superplasticizer due to its ability to enhance the workability level of fresh geopolymer concrete [19]. Several superplasticizers exist, but recent studies show sucrose is commonly used as an admixture in geopolymers because of its large availability and effectiveness in extending the setting time [20]. Hence this study uses sucrose as the admixture.

Table 13 Tensile strength of steel reinforcement

Type of Steel	Area (mm^2)	Fy (*MPa*)	Fu (*MPa*)	Elastic Modulus (*MPa*)
D16-1	193,92	481	614	200000
D16-2	193,42	478	617	200000
D16-3	192,93	473	615	200000
Average	193.42	477.33	615.33	200000
ø6-1	24,55	489	595	200000
ø6-2	24,73	461	574	200000
ø6-3	24,99	480	588	200000
Average	24.76	476.67	585.67	200000

A.6. STEEL REINFORCING BAR

Two steel reinforcing bars are used as the flexure and shear reinforcement for the beam samples. Before Casting, the steel needs to be tested by tensile strength to determine its ultimate force. Table 13 shows the tensile strength result of each type of steel.

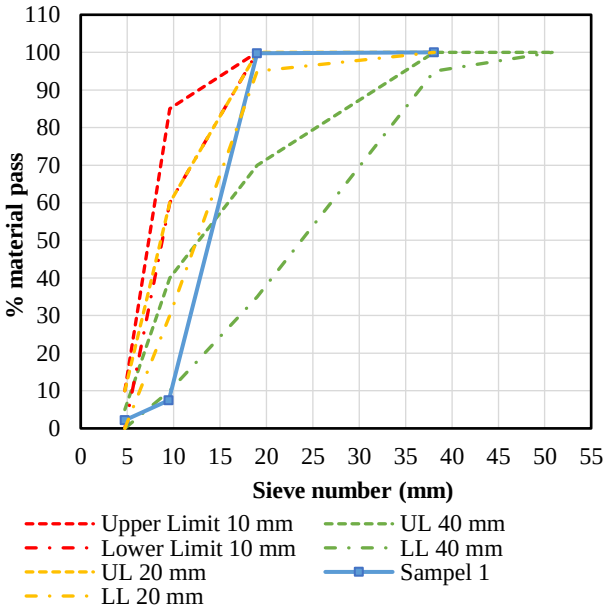

Figure 1 Sieve analysis graphic of coarse aggregates

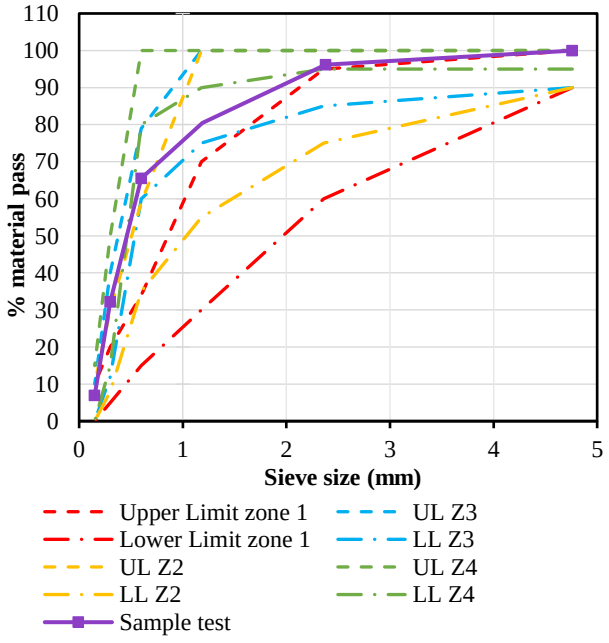

Figure 2 Sieve analysis graphic of fine aggregates

B. MIX DESIGN FORMULA

Many researchers have obtained the mix design procedures for geopolymer concrete. This study uses a mixed design procedure to achieve a compressive strength of fc' 50 MPa by 28 days [21]. The mixed design proportions are shown in Table 14.

Table 14 Mix design proportion

Mix Design		
Material	Amount (kg/m^3)	*Superplasticizer* (SP) 2% (kg/m^3)
Fly ash	669,3	669,3
Fine aggregates	450	450
Coarse aggregates	1051,5	1051,5
NaOH	133,9	133,9
Na_2SiO_3	133,9	133,9
Superplasticizer	-	13,4
Concrete density	2438,5	2451,9

C. TEST SPECIMEN

The beams observed in this research have distinguishing variables, namely a/d value, which:

a = loading span from the point load to the nearest ends
d = effective depth of the cross-section

Both beams are designed according to equation (1) to perceive the diagonal tensile cracks considered shear stress failure.

$$Pu_{flexure} > Pu_{shear} \quad (1)$$

Based on the section properties and bottom reinforcement, Pu $_{flexure}$ is calculated. Also, calculating the stirrups reinforcement achieves the value of Pu $_{shear}$. Table 15 displays the parameters of each beam observed, and Figure 3 is the detailed drawing.

Table 15 section properties of testing beams

Beam	Reinforcement			*a* (mm)	*a/d*
	Bot. Steel	Top Steel	Stirrups		
A	2 D16	2 ø6	ø6 – 250	450	2
B	2 D16	2 ø6	ø6 – 250	550	2.5

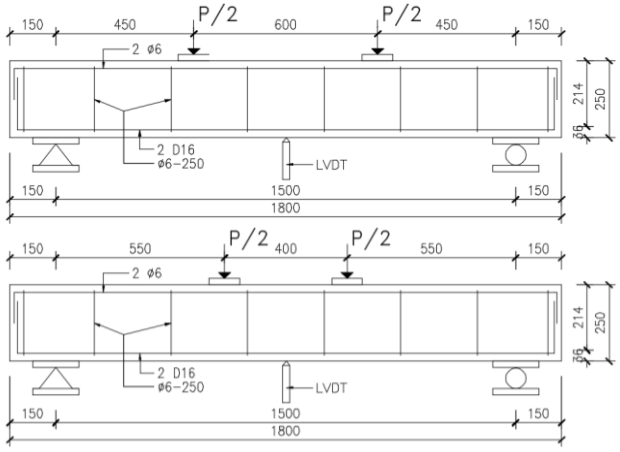

Figure 3 Beam samples A (top) and B (bottom)

D. TEST SETUP AND PROCEDURE

The testing procedure refers to ASTM C78 / C78M-15, the standard test method for the flexural strength of concrete. This test uses Universal Testing Machine as the leading equipment, but several items are also required, such as:

- Load-cell. It is a sensor designed to detect the pressure or weight of a load. It is placed on the top of the dividers' steel beam under the UTM pressure load. This device function validates the load UTM pushes to the sample, whether it works inline.
- LVDT, or Linear Variable Differential Transformer, is a displacement sensor that converts a linear position or displacement. It needs to connect with a data logger to decrypt the displacement data.
- Data Logger,
- A steel beam, usually using an H beam, distributes the load from UTM to two points to perform four-point load bending.
- Steel ball rod to give the distributed load at the accurately measured spot.

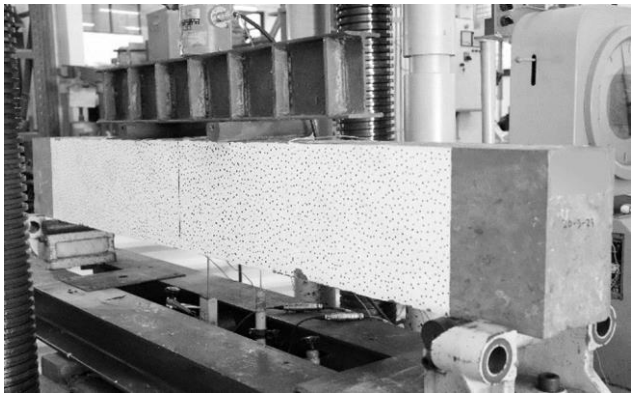

Figure 4 Four-point load bending setting test

In addition, compressive strength tests were carried out to determine the fc' value. Table 16 shows the average concrete compressive strength values for beam type A of 58,23 MPa and 59,80 MPa for beam type B.

Table 16 Compressive strength at age of 28 days

Compressive strength *f'c*	Beam A *f'c* (*MPa*)	Beam B *F'c* (*MPa*)
Sample 1	57,81	58,70
Sample 2	59,08	61,12
Sample 3	57,81	59,59
Average	58,23	59,80

RESULTS AND DISCUSSIONS

A. LOAD- DEFLECTION

The results of the Data Logger produce a peak load-deflection curve that matches the experimental results shown in Figure 5. The deflection shown in Figure 5 was measured at the mid-span using LVDT on each geopolymer-reinforced concrete beam type A and type B specimen. Each specimen that has been tested is analyzed for its peak load and deflection.

Based on the geopolymer-reinforced concrete beam tests shown in Figure 5 dan Table 17, beam type A has a peak load value of 230.07 kN, and the deflection in this

beam was 28.72 mm. Meanwhile, beam type B peak load value from the four-point bending test results was 178.01 kN with a deflection value of 23.64 mm. The deflection value of beam type A was 21.49% higher than the deflection of the beam type B. So it shows that the beam type A was more ductile than the beam type B.

Table 18 compares the peak load values of the experimental results with the results of analysis using the Response 2000 software. Table 18 shows that the comparison value of Pu Test/Pu Response 2000 on beam type A was 1.61. However, the beam type B Pu Test/Pu Response 2000 ratio was 1.30. The comparison value of Pu Test/Pu Response 2000 for each beam test object has an average ratio of 1.45 with a COV value of 10.58%.

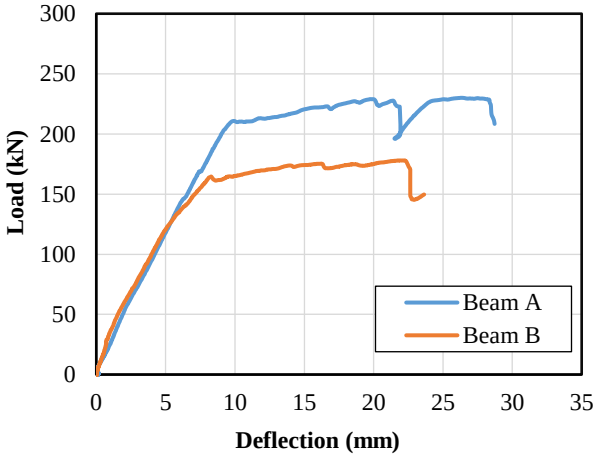

Figure 5 Load-deflection curve

Table 17 The results of the peak load and deflection values

Beam	Ultimate Load	
	P_u Test (kN)	Mid Disp. Test (mm)
A	230,07	28,72
B	178,01	23,64

Table 18 Comparison of the peak load value of the experimental results with the results of the Response 2000 analysis

Beam	Ultimate Load		P_u Test/ P_u Response 2000
	P_u Test (kN)	P_u Response 2000 (kN)	
A	230,07	143,17	1,61
B	178,01	136,98	1,30
		Mean	1,45
		COV (%)	10,58

B. CRACK PATTERN

Figure 6 and Figure 7 shows the crack patterns in geopolymer concrete with beam types A and B. The crack pattern was analyzed for the load when it experiences the first crack, the crack pattern that occurs when the reinforcement is yielding, and the shear failure in each beam specimen.

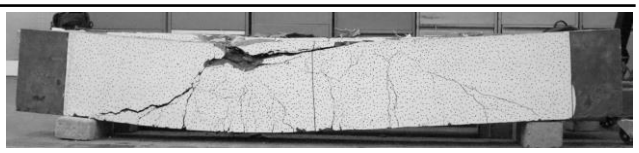

Figure 6 Crack pattern beam type A

The beam type A has the first crack in the bending area with a crack load value of 39.76 kN. After having a flexural crack, the crack spreads to the area approaching the support so that a shear crack occurs, as shown in Figure 6. The increased load on the beam causes a shear failure at the peak load of 230.07 kN. Before the shear failure, the beam crushes in the compression zone below the load location. The failure that occurs in beam type A is shear compression failure.

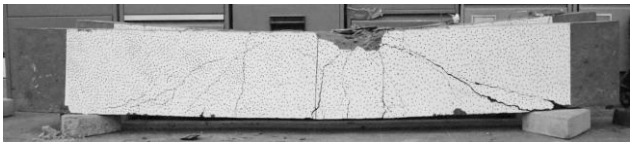

Figure 7 Crack pattern beam type B

This beam has the first crack in the bending region with a crack load value of 32.93 kN. After the first crack occurs, the crack spreads toward the support area, as shown in Figure 7. The peak load that occurs on this beam is 178.01 kN. Before the shear failure, the beam crushes in the compression zone below the loading location. Beam type B also has shear compression failure.

C. SHEAR CAPACITY

Table 19 compares the shear capacity in geopolymer concrete from the experimental results with the shear capacity of the results of analytical calculations using ACI 318-19 code. Table 19 shows that the shear capacity value of the experimental results on beam type A is 115.04 kN, and the shear capacity of beam type B is 89.00 kN. The difference in the placement of the shear span to depth ratio a/d causes a difference in the value of the shear capacity of the geopolymer beam. The a/d value of 2 has a higher shear capacity value of 29.25% than the a/d was 2.5.

Table 19 Comparison of the shear capacity of the experimental results with analytical calculations according to ACI 318-19

Beam	Shear Load		V_u Test/ V_n ACI 318-19
	V_u Test (kN)	V_n ACI 318-19 (kN)	
A	115,04	60,29	1,91
B	89,00	60,81	1,46
		Mean	1,69
		COV (%)	13,18

Furthermore, a comparison of the shear capacity of the experimental results with analytical calculations according to ACI 318-19 shows that the Vu Test/Vn 318-19 value for beam type A has a value of 1.91. however, for beam type G1B2.5, the Vu Test/Vn 318-19 comparison value is 1.46. The comparison value of the two beams has an average of 1.69, with a COV value of 13.18%. The shear capacity of the experimental results has an average value that is higher than the shear capacity value resulting from analytical

calculations according to ACI 318-19. So it can be concluded that the calculation of shear capacity using ACI 318-19 has a more conservative value.

CONCLUSIONS

This paper has presented the results of experimental testing of geopolymer concrete beams using high calcium fly ash with variations in a/d loading locations. The beam types A and B were tested for four-point bending according to the a/d loading location. The results of the discussion carried out are the deflection load curve, the comparison of the peak load of the experimental results with the response of 2000, the pattern of cracks that occur in each specimen, and the comparison of capacities that occur as a result of experiments with analytical calculations according to ACI 318-19. So the conclusions that can be drawn from this study are as follows.

1. The comparison of the peak load-deflection curves of beam type A and beam type B shows that beam type A is more ductile than beam type B, with a percentage difference of about 21.49% in deflection.
2. Comparison of the peak load value of the experimental results with analysis using response 2000 has an average value of 1.45 with a COV value of 10.58%.
3. The shear failure that occurs in beams of type A and B is shear compression failure.
4. The shear capacity of beam type A has a higher value of 29.25% than beam type B. So the a/d value is inversely proportional to the shear capacity value.
5. The shear capacity of the experimental test results on beams of type A and B has a higher value than the calculation of the shear capacity using ACI 318-19 code with an average ratio of 1.69 and a COV of 13.18%. So it can be concluded that the calculation of shear capacity using ACI 318-19 code is more conservative because it considers it from a safety perspective.

ACKNOWLEDGMENTS

This study has been funded by Beasiswa Pendidikan Indonesia (BPI) from Kementerian Pendidikan, Kebudayaan, Riset, dan Teknologi (Kemdikbudristek) and Lembaga Pengelola Dana Pendidikan (LPDP), Indonesia.

REFERENCES

[1] N. P. Rajamane, M. C. Nataraja, and N. Lakshmanan, “An introduction to geopolymer concrete,” *Indian Concrete Journal*, vol. 85, no. 11, pp. 25-28, November, 2011.

[2] B. C. Mclellan, R. P. Williams, J. Lay, A. Van Riessen, and G. D. Corder, “Costs and carbon emissions for geopolymer pastes in comparison to ordinary portland cement,” *Journal of Cleaner Production*, vol. 19, no. 9–10, pp. 1080–1090, 2011, doi: 10.1016/j.jclepro.2011.02.010.

[3] R. J. Flatt, N. Roussel, and C. R. Cheeseman, “Concrete : An eco material that needs to be improved,” *Journal of the European Ceramic Society*, vol. 32, pp. 2787–2798, 2012, doi: 10.1016/j.jeurceramsoc.2011.11.012.

[4] E. Gartner and H. Hirao, “Cement and Concrete Research A review of alternative approaches to the reduction of CO 2 emissions associated with the manufacture of the binder phase in concrete,” *Cement and Concrete Research*, 2015, doi: 10.1016/j.cemconres.2015.04.012.

[5] B. Singh, G. Ishwarya, M. Gupta, and S. K. Bhattacharyya, “Geopolymer concrete : A review of some recent developments,” *Construction and Building Materials*, vol. 85, pp. 78–90, 2015, doi: 10.1016/j.conbuildmat.2015.03.036.

[6] M. Venu and T. D. Gunneswara Rao, “An Experimental Investigation of the Stress-Strain Behaviour of Geopolymer Concrete,” *Slovak Journal of Civil Engineering*, vol. 26, no. 2, pp. 30–34, Jun. 2018, doi: 10.2478/sjce-2018-0011.

[7] Y. N. Wibowo, B. Piscesa, and Y. Tajunnisa, “Numerical Investigation of Geopolymer Reinforced Concrete Beams Under Flexural Loading Using Finite Element Analysis,” *Journal of Civil Engineering*, vol. 37, no. 1, 2022.

[8] M. W. Aziz, P. Suprobo, and Y. Tajunnisa, “Numerical Analysis Study of The Effect Geopolymer Concrete Compressive Strength on Ductility of Reinforced Concrete Beams,” *Journal of Civil Engineering*, vol. 37, no. 1, p. 33, 2022.

[9] Januarti Jaya Ekaputri and Triwulan, “Geopolymer Concrete Using Fly Ash, Trass, Sidoarjo Mud Based Material,” *Journal of Civil Engineering*, vol. 31, no. 2, 2011.

[10] T. Glasby, J. Day, R. Genrich, and M. Kemp, “Commercial scale geopolymer concrete construction,” in *The Saudi International Building and Constructions Technology Conference*, pp. 1–11, 2015

[11] Y. Tajunnisa, M. Sugimoto, T. Sato, J. Jaya, and M. Shigeishi, “Characterization of low calcium,” in *16th International Conference and Exhibition on Structural Faults and Repair*, 2016.

[12] Y. Tajunnisa, M. Sugimoto, T. Uchinuno, and T. Sato, “Performance of alkali-activated fly ash incorporated with GGBFS and micro-silica in the interfacial transition zone , microstructure , flowability , mechanical properties and drying shrinkage,” in *AIP Conference Proceedings*, 2017. doi: 10.1063/1.5003517.

[13] Y. Tajunnisa, M. Sugimoto, T. Sato, M. Shigeishi, and C. Author, “A study on factors affecting geopolymerization of low calcium fly ash,” *International Journal of GEOMATE*, vol. 13, no. 36, pp. 100–107, 2017.

[14] R. Bayuaji, M. S. Darmawan, and N. A. Husin, “Utilization of High Calcium Content Fly Ash : Flexural Strength of Geopolymer Utilization of High Calcium Content Fly Ash : Flexural Strength of Geopolymer Concrete Beams in Sea Water Environment,” *The Open Civil Engineering Journal*, vol. 10, no. December, pp. 782–793, 2016, doi: 10.2174/1874149501610010782.

[15] T. Xie, P. Visintin, X. Zhao, and R. Gravina, "Mix design and mechanical properties of geopolymer and alkali activated concrete : Review of the state-of-the-art and the development of a new unified approach," *Construction and Building Materials*, vol. 256, p. 119380, 2020, doi: 10.1016/j.conbuildmat.2020.119380.

[16] A. Hosan, S. Haque, and F. Shaikh, "Compressive behaviour of sodium and potassium activators synthetized fly ash geopolymer at elevated temperatures: A comparative study," *Journal of Building Engineering*, vol. 8, pp. 123–130, 2016, doi: 10.1016/j.jobe.2016.10.005.

[17] G. S. Ryu, Y. B. Lee, K. T. Koh, and Y. S. Chung, "The mechanical properties of fly ash-based geopolymer concrete with alkaline activators," *Constr. Build. Mater*, 2013, doi: 10.1016/j.conbuildmat.2013.05.069.

[18] ASTM, *AASTM C 33 - 03 Standard Specification for Concrete Aggregates*, vol. 04. 2001.

[19] H. Haji-Esmaelii, *Admixtures for use in geopolymers*. 2012.

[20] T. A. Bhat, R. Kumar, M. A. Dar, and J. Raju, *Effect of sugarcane molasses on properties of geopolymer concrete*, vol. 1, no. 2006. Springer International Publishing, 2019. doi: 10.1007/978-3-030-02707-0.

[21] T. Phoo-ngernkham, C. Phiangphimai, N. Damrongwiriyanupap, S. Hanjitsuwan, J. Thumrongvut, and P. Chindaprasirt, "A mix design procedure for alkali-activated high-calcium fly ash concrete cured at ambient temperature," *Advances in Materials Science and Engineering*, vol. 2018, 2018.